

## Modeling Inverter Losses for Circuit Simulation

A. FRATTA AND F. SCAPINO

Department of Electrical Engineering  
Politecnico di Torino  
Corso Duca degli Abruzzi 24, 10129, Torino, Italy  
e-mail: scapino@polito.it

**Abstract**— Transformer-like inverter models can represent a very good alternative to common switch-diode models for simulation, reducing convergence problems and/or calculation time. They may also provide easier insight into the converter operation and power loss effects, at least from the point of view of the applicants, aiding for design and teaching purposes.

The paper shows how conduction and switching losses can be incorporated in the transformer-like inverter model in a simple and intuitive way, which requires very few parameters and allows for separate modeling of lossless behavior, conduction losses and the switching losses. Loss models are proposed in some versions differing for the accuracy and simulation easiness. In any case, the resulting inverter lossy model is very compact and can be implemented by just a pair of nonlinear controlled sources as basic building blocks, available in any circuit simulation program, as the free of charge and widely used PSpice Student Version.

### I. INTRODUCTION

The switched-mode converters may be simulated by accurate replacement of each power device with its model, available in custom libraries for circuit simulators. On the other hand this is extremely calculation-time consuming, since very many and very fast phenomena would be simulated.

An easier simulation concept, applicable to IGBT power modules simulation, takes care of replacing all the active devices with diodes and controlled switches [1]. Besides the inaccuracy, at least for commutation losses, this approach may generate simulation convergence problems as well. Furthermore it does not provide intuitive understanding and evaluation of power loss performance, as it would be useful both in design and education areas. In addition, due to the increasing use of distributed non conventional DC power sources, such as photovoltaic generators and fuel cells, whose efficiency is greatly influenced by their operating point, a simple inverter model that holds the interaction between AC and DC sides would be highly desirable.

To overcome these limits and meet these needs, a two-port transformer-like model for the whole inverter, has been derived from power balance considerations (PBIM) [2]. It is ready to implement in any circuit simulation environment using only one pair of controlled sources, without any need for junction devices and offers several remarkable advantages in simulation at various levels of accuracy, from lossless behavior to averaged and instantaneous simulation

of both conduction and switching losses, separately modeled.

The model is proposed in three different versions using the same structure and parameters set: the most general is able to model the lossy behavior of inverters operating with any switching function -also at variable frequency-; the second is restricted to inverters working at fixed switching frequency and the last requires, in addition, that the voltage and current waveform have a simple analytical formulation, as in the case of sinusoidal PWM, and coincides with the so-called averaged switch model [3,4,5,6].

### II. LOSSY MODEL OF THE INVERTER LEG

#### A. VSI leg lossless model

A PWM canonical cell of commutation is depicted in Fig. 1a as a common inverter leg power module, represented by a two-port net and highlighting the ports variables.

The ideal behavior of the circuit, in which all the components are “non-energetic” circuit elements [7], shows a perfect balance of the port instantaneous powers:

$$v_1(t)i_1(t) = -v_2(t)i_2(t) \quad (1)$$

With reference to the widely adopted class of Voltage Source Inverters (VSI), the generation of the output voltage is expressed in (2) by means of the port voltage relationship:

$$v_2(t) = r(t) \cdot v_1(t) \quad (2)$$

where  $r(t)$  is a binary rectangular function, thus switching between the values “0” and “1”.

According to possible PWM techniques and AC load application, the binary function may be usefully substituted by the instantaneous modulation index  $s(t)$  as in (3), switching between the opposite values “-1” and “+1”:

$$r(t) = \frac{1+s(t)}{2} \quad (3)$$

Equation (1) and (2) lead to the characterization of the ideal two-port element according to (4):

$$\begin{bmatrix} v_1(t) \\ i_1(t) \end{bmatrix} = \begin{bmatrix} 1/r(t) & 0 \\ 0 & r(t) \end{bmatrix} \begin{bmatrix} v_2(t) \\ -i_2(t) \end{bmatrix} \quad (4)$$

This lossless model can be associated to a time-varying ideal transformer, whose “turns ratio” is given by  $1/r(t)$  as

reported in Fig. 1b. It is worth noting that analogous relation holds for the complementary class of Current Source Inverters (CSI).

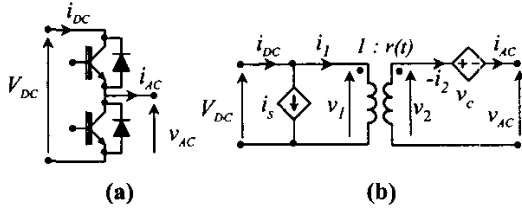


Fig. 1. The switch-mode inverter leg and its port variables (a). The transformer-like model consisting of a time-varying ideal transformer and two lossy elements (b).

**B. VSI leg conduction losses model**

Conduction losses can be modeled by a voltage source  $v_c$ , that accounts for the voltage drop on each conducting device, connected in series to the transformer secondary side as suggested in Fig. 1b. It represents the difference between the ideal and the actual AC-side voltage as stated by the relation:

$$v_c = r(t) \cdot V_{DC} - v_{AC} \tag{5}$$

The value and the polarity of this voltage drop depend on the direction of the alternating current (i.e. on the active elementary cell) and on the leg transistors control signal  $r(t)$  that determines the conduction path (transistor or diode of the active cell).

The following table can easily summarize all possible combinations:

TABLE I  
CONDUCTION VOLTAGE DROP

	$r = 1 \quad (s = +1)$	$r = 0 \quad (s = -1)$
$i_{AC}(t) > 0$	$V_T$	$V_D$
$i_{AC}(t) < 0$	$-V_D$	$-V_T$

From this table, the analytical expression (6) is immediately derived:

$$v_c = \text{sign}(i_{AC}) \cdot [wV_T + (1-w)V_D] \tag{6}$$

being  $w$  the logic function defined in (7):

$$w = \frac{1 + \text{sign}(i_{AC}) \cdot s(t)}{2} \tag{7}$$

Substitution of (7) in (6) points out in (8) how average and differential voltage drops affect conduction losses with respect to individual transistor and diode characteristics:

$$v_c = \text{sign}(i_{AC}) \cdot \frac{V_T + V_D}{2} + s(t) \cdot \frac{V_T - V_D}{2} \tag{8}$$

Note that the “common-mode” of the I-V characteristics is not affected by the switching function, affecting only their “differential-mode”.

A piecewise linear approximation for both transistor and

diode I-V characteristics is usually adopted (open-circuit voltage  $V_{X0}$  and series resistance  $R_X$ ).

In the case, (8) can be further developed for easy implementation in a circuit simulation program:

$$v_c = v_A + v_S \tag{9a}$$

where:

$$v_A = \frac{V_{T0} + V_{D0}}{2} \cdot \text{sign}[i_{AC}(t)] + \frac{R_T + R_D}{2} \cdot i_{AC}(t) \tag{9b}$$

shows the effects of common-mode terms, and:

$$v_S = \left[ \frac{V_{T0} - V_{D0}}{2} + \frac{R_T - R_D}{2} \cdot |i_{AC}(t)| \right] \cdot s(t) \tag{9c}$$

points-out the impact of the switching index  $s(t)$ .

**C. VSI leg switching losses model**

The switching losses of common medium power modules are synthetically specified in terms of the switching energies  $E_{on}$  and  $E_{off}$ , measured for clamped inductive load. They depend on the driving circuit and can be considered (to a first approximation) proportional to the DC voltage and to the instantaneous value of AC current [8]. Therefore by dividing them by the test voltage and current, two equivalent time commutation constants can be obtained, characterizing the transistors turn-on and turn-off effects:

$$T_{EQON} = \frac{E_{ON}}{V_{TEST} \cdot I_{TEST}}; T_{EQOFF} = \frac{E_{OFF}}{V_{TEST} \cdot I_{TEST}} \tag{10a, 10b}$$

Using the previous definitions, the area of the pulses of power lost in correspondence of the transistor turn-on and turn-off, can be expressed as:

$$E_{SPON} = T_{EQON} \cdot V_{DC} \cdot |i_{AC}(t)| \tag{11a}$$

$$E_{SPOFF} = T_{EQOFF} \cdot V_{DC} \cdot |i_{AC}(t)| \tag{11b}$$

From the above considerations, switching losses can be modeled by means of a pulsed current generator, in parallel to the ideal transformer primary side. Although the proposed model does not pretends to exactly reflect the physical situation, this choice is justified by the consideration that many of the phenomena involved into the switching mechanism (diode reverse recovery, transistor tail, transition of the transistor operating point trough the active region) imply a charge transfer on an equivalent non-linear capacitance connected across the DC bus.

These current pulses account for the difference between the actual and the ideal shapes of the DC-side current:

$$i_s = i_{DC} - r(t) \cdot i_{AC} \tag{12}$$

In a very simple circuitual model, they are obtained from the  $r(t)$  (or  $s(t)$ ) switching function by means of two first order high-pass filters, whose time constants are precisely  $T_{EQON}$  and  $T_{EQOFF}$ . These high-pass filters generate two

trains of bipolar pulses having areas proportional to  $T_{EQON}$  and  $T_{EQOFF}$ , respectively, not depending on  $r(t)$  transition times.

These pulse trains are multiplied by  $i_{AC}(t)$  and its opposite, respectively, and, after the cancellation of the negative pulses, are summed up as in (13):

$$i_s = \text{Max} \left[ 0, i_A(t) \cdot L^{-1} \left\{ R(p) \frac{pT_{EQON}}{1+pT_{EQON}} \right\} \right] + \text{Max} \left[ 0, -i_A(t) \cdot L^{-1} \left\{ R(p) \frac{pT_{EQOFF}}{1+pT_{EQOFF}} \right\} \right] \quad (13)$$

where the filters transfer function is multiplied by the Laplace transform of  $r(t)$ :

$$R(p) = L\{r(t)\} \quad (14)$$

Expression (13) is easy explained observing that, during the positive modulation half-period, transistor turn-on and turn-off take place in correspondence to the rising and falling edges of  $r(t)$ , while the opposite correspondence hold, during the negative modulation half-period.

The accuracy of the above expressions is satisfactory in many applications, taking into account the uncertainty of all parameters. However more precise analytical functions of the switching losses could be chosen, as an example adding square terms of DC voltage and also of load current.

The current pulse train (13) makes it possible to account for switching losses by real time and at the highest accuracy, thanks to well-defined areas calculated at the actual values of all variables. This is why the simulation (13) is generally applicable for all PWM techniques, also in those circuits operating at variable switching frequency, as in case of hysteretic regulation. In addition, the waveform of (13) on the DC current  $i_{DC}(t)$  increases the accuracy of the whole simulation. As a main drawback, a simulation step ceiling is required to achieve simulation accuracy according to steep waveform edges.

For faster calculation time, whenever the inverter operates at fixed switching frequency  $f_s=1/T_s$ , the energy lost in each switching period  $T_s$  can be simulated by less discontinuous shapes of  $i_s(t)$  while holding the average value.

As an example, current pulses of  $i_s(t)$  synchronous with the primary current pulses are provided according to (15):

$$i_s = \frac{T_{EQ}}{T_s \cdot \langle r(t) \rangle_{T_s}} \cdot |r(t) \cdot i_A(t)| \quad (15)$$

being:

$$T_{EQ} = T_{EQON} + T_{EQOFF} \quad (16)$$

At fixed PWM frequency the fastest calculation times are achieved by means of continuous functions and a further simplification is possible by replacing all the time-varying

functions with their value averaged over the switching period. In this case, the model coincides with the so-called averaged switch model [5]. In particular expression (15) simply becomes:

$$i_s = \frac{T_{EQ}}{T_s} \cdot |i_A(t)| \quad (17)$$

Obviously this model is less accurate and can be used in those applications where knowing the average circuit behavior is acceptable, that are where PWM ripples and their effects are low with respect to main average effects. This is the case in most of the medium-power applications.

#### D. Leg losses averaged over one modulation period

Averaged and continuous simple analytical expressions are found by integration of the instantaneous formulations over one period, by holding constant suitable variable values in each switching (and integration) period. This is the only simplifying hypothesis and all error is related to it.

As example for VSI applications, this is equivalent to neglect the PWM ripples, on AC-side current and on the DC-link voltage.

In the case, integration of (9) and (17) over one modulation period leads to (18,19), that provide the expressions of conduction and switching losses, respectively, valid for an inverter leg supplying sine load current:

$$P_{CLEG} = \frac{V_{T0} + V_{D0}}{\pi} \hat{I}_{AC} + \frac{R_{T0} + R_{D0}}{4} \hat{I}_{AC}^2 + 2m \cos \varphi \left( \frac{V_{T0} - V_{D0}}{8} \hat{I}_{AC} + \frac{R_{T0} - R_{D0}}{3\pi} \hat{I}_{AC}^2 \right) \quad (18)$$

$$P_{SLEG} = \frac{2}{\pi} f_s T_{EQ} V_{DC} \hat{I}_{AC} \quad (19)$$

being  $m$  is the modulation index and  $\varphi$  the leading angle of the fundamental component of  $s(t)$  with respect to the AC current, having  $\hat{I}_{AC}$  peak amplitude.

These well-known expressions are of practical use in dimensioning the power devices heatsink [9].

### III. INVERTER LOSSY MODELS

The different modeling levels are described above for a single canonical PWM cell.

Particularly in the case of VSIs, these ones are directly applicable to multiphase inverters, by simple composition. As main examples, models of various inverter topologies can be easily built up as done in Fig.2a, 2b, and 2c, for the most common structures of VSIs. Here the unitary amplitude alternating function  $s(t)$  appears in the ideal transformer turns ratio of all the inverter topologies, due to AC voltage requirement.

Where the transformer simulates a single leg, the turns ratio shows the number "2" at primary side, taking into

account that the effective AC voltage range of a single phase leg is  $\pm 1/2 V_{DC}$  that is the cell voltage with respect to the mid-point potential of the DC-link supply voltage.

In the case the mid-point is generated by series capacitors, the two capacitors appearing in the single-phase half-bridge inverter equivalent circuit account for the effects of such capacitive voltage divider on both DC and AC sides.

Note also that, for the single-phase full-bridge inverter model, in case of bipolar modulation scheme it is:

$$s_2(t) = -s_1(t)$$

Therefore, the ideal transformer turns-ratio of the full-bridge bipolar inverter reduces to:

$$n(t) = s_1(t)$$

and, bearing in mind that for the output current of the two inverter legs it is:

$$i_{AC2}(t) = -i_{AC1}(t)$$

the voltage source accounting for the inverter conduction losses becomes:

$$v_{c1} - v_{c2} = 2v_A + 2v_s$$

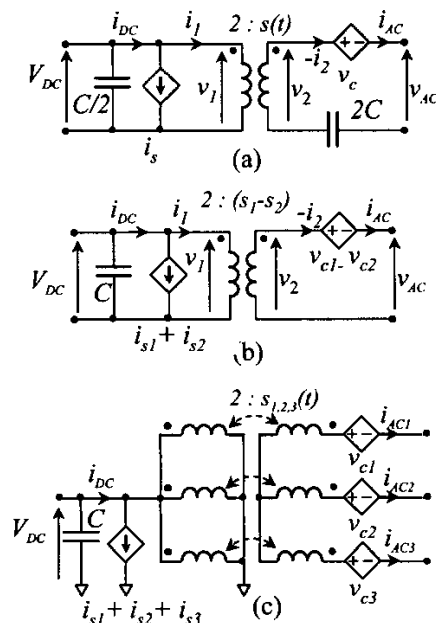


Fig.2. The main inverter topologies. Equivalent circuit of a single-phase half-bridge application (a), single-phase full-bridge (b) and three-phase (c)

#### IV. SIMULATIONS EXAMPLES OF CIRCUITS CONTAINING INVERTERS

In order to show some meaningful application of the proposed models, a practical application is considered in which a photovoltaic (PV) generator is connected to the utility grid through a full-bridge VSI, a decoupling inductor and a line-frequency insulation transformer.

The PV generator is constituted by the parallel connection of two strings of 18 standard modules and exhibits an open-circuit voltage and a short circuit current (at standard

irradiance condition –  $G=1kW/m^2$ -):

$$V_{OC}=400V; I_{SC}=10A.$$

The VSI is an H-bridge IGBT inverter built up with two leg modules SK25GB023 (600V, 30A max ratings)

It must be controlled by means of a current loop in order to inject a current of desired peak value into the grid at unitary PF. The loop reference signal is set to a value that forces the PV generator to work near to the maximum power point [10].

Simulations presented here refer to two different ways suitable to this goal:

- 1) operation in the bipolar PWM mode, at fixed switching frequency;
- 2) operation at variable switching frequency under hysteretic control.

Fig. 3 shows the PSpice schematic diagram of the overall circuit. In the top figure the model of the above described reference power system is drawn, where the inductor  $L_{AC}$  accounts for both the decoupling and the parasitic inductances, the resistor  $R_{AC}$  collects the series conduction losses of the AC side components and  $v_{GRID}(t)$  is the open-circuit grid voltage “seen” by the inverter. The PV generator is modeled by a real voltage source (open-circuit voltage  $V_{OC}=400V$  and series resistance  $R_S=5\Omega$ ) with current limit ( $I_{SC}=10A$ ).

The values of the circuit components are:

$$C=2.2mF, R_{AC}=0.3\Omega, L_{AC}=2.5mH \text{ and } V_{GRID} = 230V_{rms}.$$

The inverter operates in PWM bipolar mode ( $f_s=10 \text{ kHz}$ ) and, here, it is simulated using the instantaneous-value model, with the following parameters values:

$$V_{T0}=0.9V, R_T=52m\Omega, V_{D0}=0.75V, R_D=30m\Omega;$$

$$T_{EQON}\cong 0.258\mu s, T_{EQON}\cong 0.108\mu s.$$

The schematic diagram shown in the bottom of the same figure refers to the functional blocks that implement the current loop and the pulsed current generator, responsible for switching losses.

The current loop is designed to limit the maximum current ripple to a value:  $\Delta I_{max}\cong 20\%$ .

Fig. 5 reports the waveforms obtained by the PSpice transient simulation of the circuit described in Fig. 3, while in Fig. 6 the results of the simulation of the same circuit using the inverter average-value model are reported for comparison purpose. As it can be seen, in the second case both conduction and switching losses are lower since contribution from high order harmonics is disregarded by the average-value model.

As an implementation alternative to be considered in the design phase, in Fig. 4 the schematic diagram of the same reference power circuit under hysteretic control is drawn.

The comparator hysteresis band has been set in order to obtain a current ripple  $\Delta I\cong 10\%$  that gives rise to inverter losses comparable to those obtained with PWM operation, as it is shown by the energies plots of Fig. 7, that reports the simulation results.

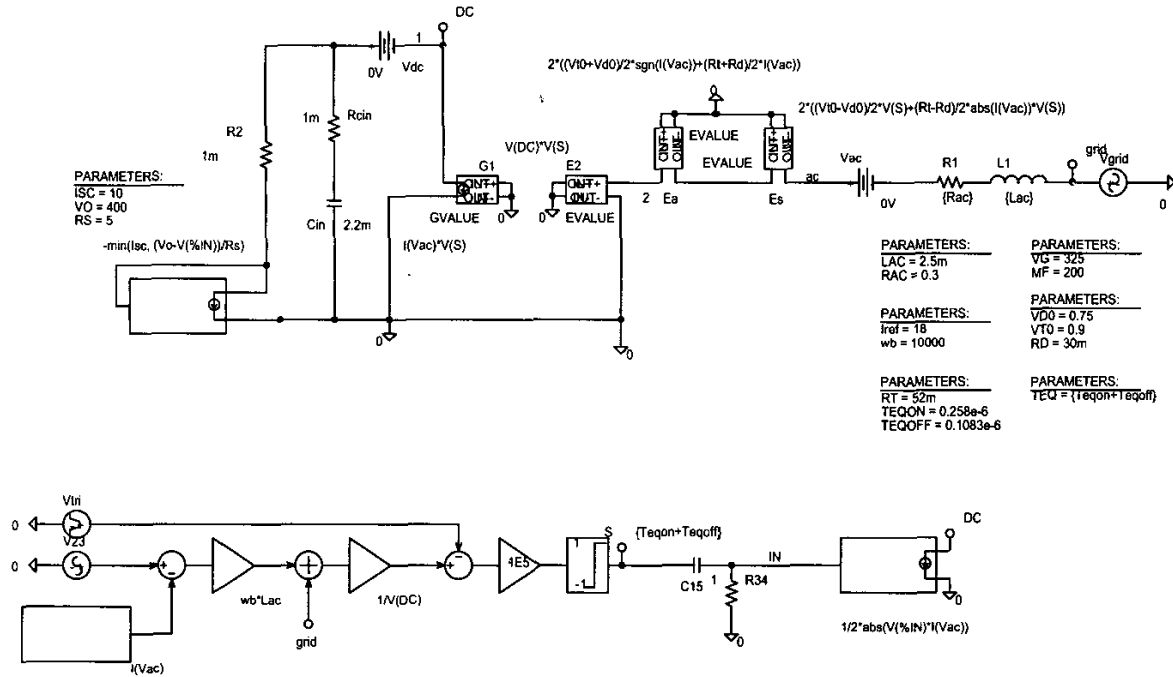


Fig. 3. PSpice simulation model. In the top figure the power system constituted by a PV generator connected to the utility grid by means of an H-bridge IGBT VSI operated in bipolar mode (here simulated with the instantaneous-value model). In the bottom the PWM modulator controlled by the current loop and the pulsed current generator accounting for switching losses.

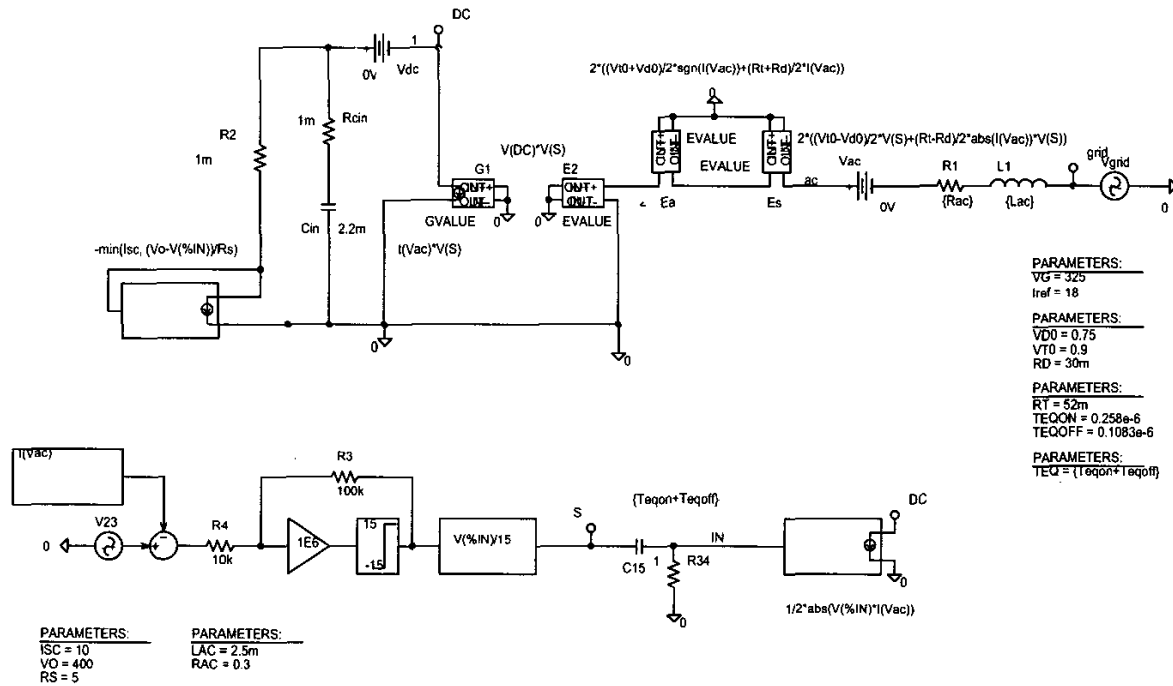


Fig. 4. PSpice simulation model of the same power system of Fig. 3 with hysteretic control. The comparator hysteresis band has been set in order to give rise to inverter losses comparable with the PWM case.

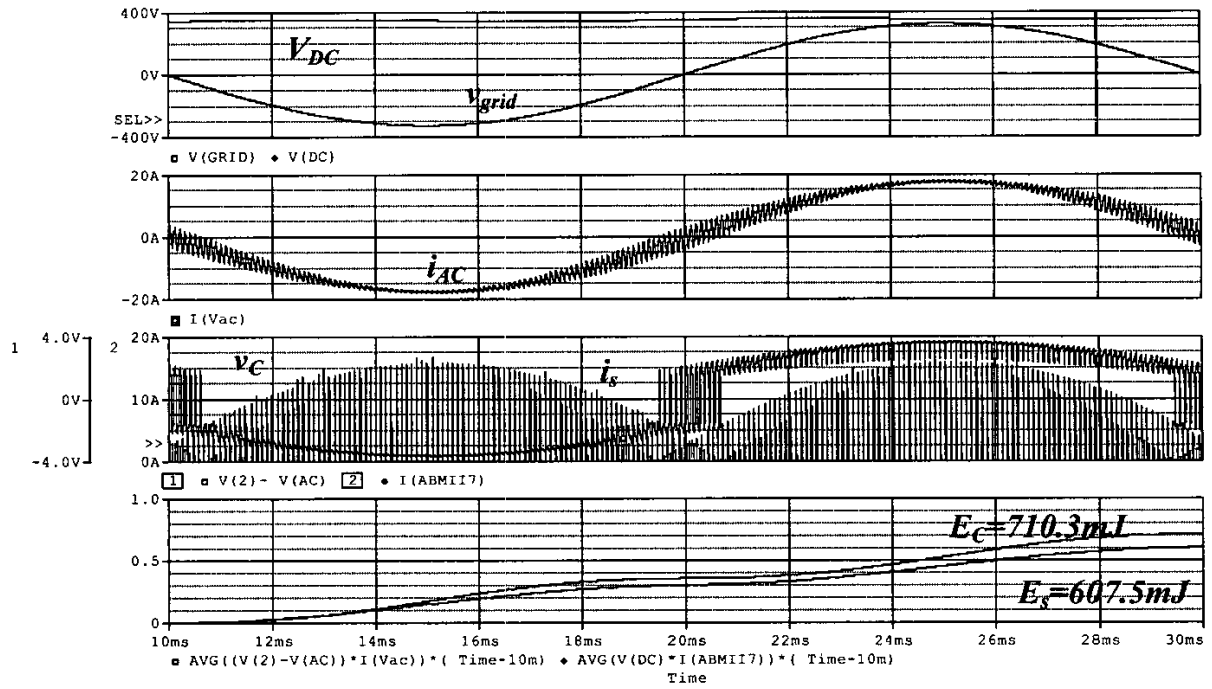


Fig. 5. PSpice simulation waveforms of the reference power system with instantaneous-value lossy model for the inverter controlled in PWM bipolar mode. From the top to the bottom panel: 1) DC and Grid voltages; 2) AC current; 3) conduction voltage drop “ $v_c$ ” and switching current “ $i_s$ ”; 4) conduction and switching energies cumulated over one modulation period.

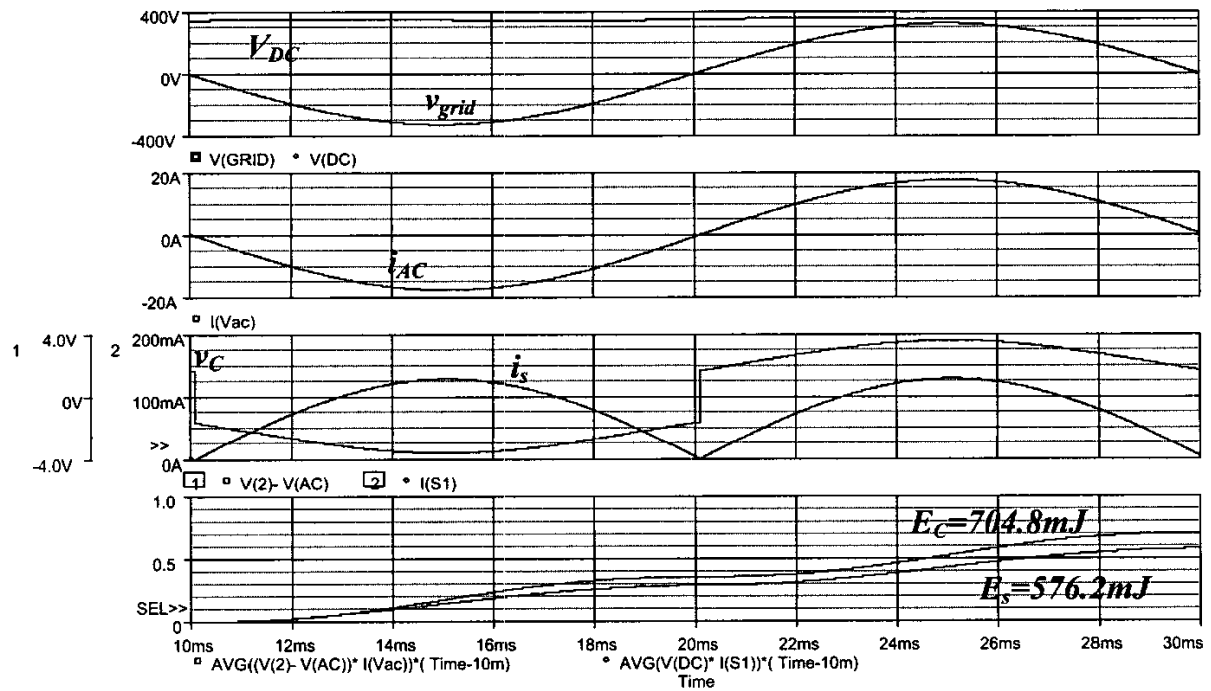


Fig. 6. PSpice simulation waveforms of the reference power system with average-value lossy model for the inverter controlled in PWM bipolar mode. From the top to the bottom panel: 1) DC and Grid voltages; 2) AC current; 3) conduction voltage drop “ $v_c$ ” and switching current “ $i_s$ ”; 4) conduction and switching energies cumulated over one modulation period.

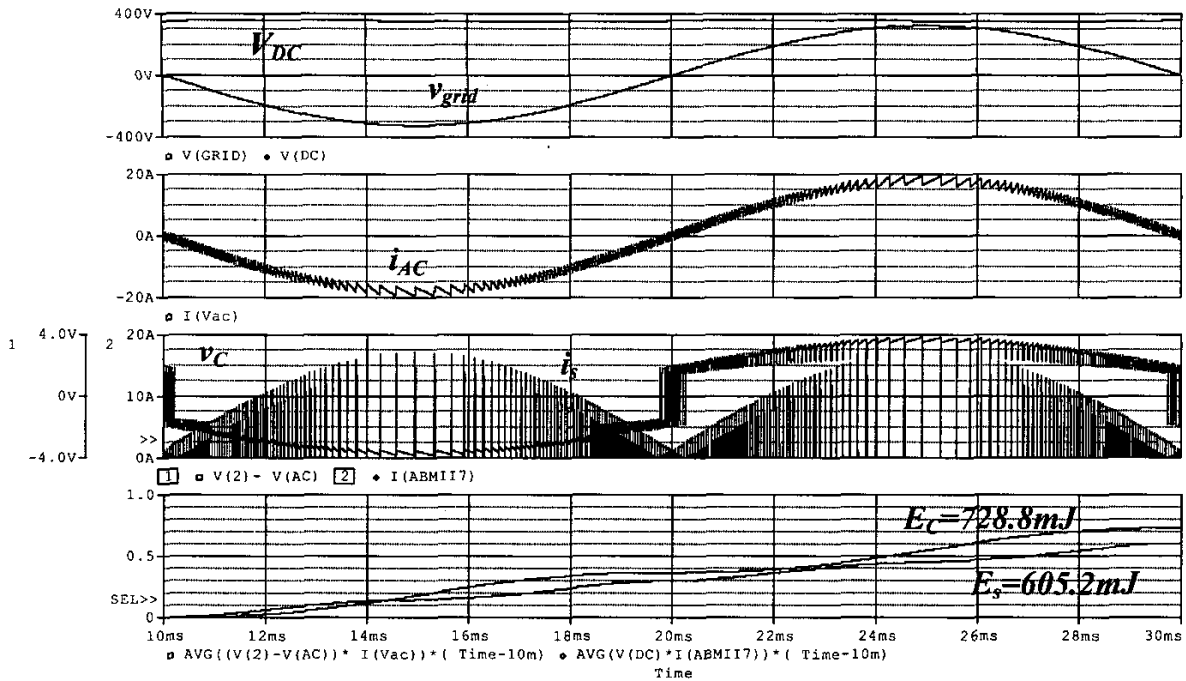


Fig. 7. PSpice simulation waveforms of the reference power system with instantaneous-value lossy model for the inverter controlled by hysteresis comparator. From the top to the bottom panel: 1) DC and Grid voltages; 2) AC current; 3) conduction voltage drop " $v_c$ " and switching current " $i_s$ "; 4) conduction and switching energies cumulated over one modulation period.

## V. CONCLUSIONS

The transformer-like model for switched-mode inverter, derived from power balance considerations on the inverter leg, allows simple separate modeling of lossless behavior, conduction and switching losses. In addition, the lossy behavior can be modeled at different accuracy degrees using the same model structure and the same set of six parameters that are easy to obtain from manufacturers data sheets. The model requires just a pair of non-linear controlled source and can be easily implemented in any circuit simulation program, as the free of charge and widely used PSpice Student Version. It can be used to simulate the behavior of inverters controlled by any kind of switching function (square-wave, PWM with any modulation scheme as well as generated by hysteretic control), as it has been shown in the simulation examples proposed in the paper. Holding the interaction between the AC and DC sides, it is, as well, a very useful tool to determine the DC generator operating point and to check its dependence on the AC load, that is a crucial issue to maximize the system efficiency when the DC power source exhibits highly non-linear I-V characteristic, as it is the case of PV generators and fuel cells. Moreover in the education area, due to its simple conceptual derivation, it helps to easily explain the converter waveforms and gives physical insight into the converter operation and design criteria.

## REFERENCES

- [1] Mohan, N., Undeland, T. M., Robbins, W. P., *Power electronics*, New York, J. Wiley & Sons, 1995.
- [2] Scapino, F., "A transformer-like model for the DC/AC converter", Proc. of IEEE ICIT 2003, Maribor, Slovenia, November 10-12, 2003, pp. 625-630.
- [3] Vorperian, V., "Simplified analysis of PWM converters using model of PWM switch. Parts I: Continuous Conduction Mode", IEEE Trans. on Aerospace and Electronic Systems, Vol. 26, pp. 490-496, 1990.
- [4] Vorperian, V., "Simplified analysis of PWM converters using model of PWM switch. Parts II: Discontinuous Conduction Mode", IEEE Trans. on Aerospace and Electronic Systems, Vol. 26, pp. 497-505, 1990.
- [5] Erickson, R. W., Maksimovic, D., *Fundamentals of power electronics*, Dordrecht, Kluwer, 2001.
- [6] Al-Naseem, O., Erickson, R. W., "Prediction of switching loss variation by averaged switch modeling", Proc. of APEC 2000, Feb 6-10, 2000, vol.1, pp. 242-248.
- [7] Chua, L. O., Desoer, C. A., Kuh, E. S., *Linear and Nonlinear Circuits*, New York, McGraw-Hill, 1987.
- [8] International Rectifier Corp, "IGBT Characteristics", AN-983.
- [9] <http://www.semikron.com>
- [10] Scapino, F., Spertino, F., "Load Curves at DC Inverter Side: a Useful Tool to Predict Behavior and Aid the Design of Grid-connected Photovoltaic Systems", Proc. of IEEE ISIE 2002, L'Aquila, Italy, July 8-11, 2002, vol. 3, pp. 981-986.